

Low polarization on-axis three-mirror reflective optical systems initial configuration designed by genetic algorithms

Jing Luo ^{a,*}, Tianxiao Xu ^{a,b}, Xu He ^a, Xiaohui Zhang ^a

^a Changchun Institute of Optics, Fine Mechanics and Physics, Chinese Academy of Science, Changchun, Jilin 130033, China

^b University of Chinese Academy of Sciences, Beijing 100049, China

ABSTRACT

Low polarization systems have important advantages in many applications. Thanks to be with seven free design parameters, three-mirror reflective systems have good potential to achieve low polarization. A general method to design low polarization on-axis three-mirror systems is proposed in this paper. Based on genetic algorithms, the initial configurations of on-axis three-mirror systems with both low polarization aberrations and good wave aberrations can be found. In order to make the design results meet different requirements, various constraints are included in the merit functions, such as diattenuation, retardance, wave aberrations, structure size, intermediate image plane and flat focal plane. Different merit functions generate different optimal results. The method proposed in this paper is versatile and can be used to design other types of optical systems that demand low polarization.

1. Introduction

Due to the ability of correcting spherical aberration, coma and astigmatism at the same time, three-mirror reflective optical systems can achieve excellent optical performance. With the advantages of being free of chromatic aberrations, compact volume, loose heat tolerance and large field of view (FOV), three-mirror reflective optical systems are widely used in many applications, such as astronomical observations [1–5], space investigation camera [6], remote sensing [7,8], and so on.

On-axis three-mirror systems, whose aperture center of optical elements coincides with their optical axis, are important members of three-mirror systems. The elements in on-axis three-mirror systems are rotationally symmetric, which is critical to many polarization-sensitive applications [9–13]. Polarization-sensitive systems include those requiring very accurate irradiance measurements and those where polarization is the intended measurement. Although wavefront errors are usually more important than polarization aberrations, polarization aberrations are inevitable for almost all optical systems [14–16]. Polarization aberrations would induce several significant effects on the performance of optical systems including retardance, diattenuation, polarization crosstalk, amplitude and phase apodization [17–20]. Breckinridge et al. have made important and detailed analyses on polarization aberrations in an on-axis telescope [18]. Polarization aberrations of on-axis and off-axis three-mirror systems have been analyzed and compared systematically in our previous work [9].

In order to reduce the effects of polarization aberrations, polarization calibration is usually adopted. However, it is a really hard work to calibrate the polarization properties of telescopes with large aperture.

Many polarization calibrations rely on specific targets, such as water cloud and ice cloud [21]. Unfortunately, the existence of these goals is unstable. What is more, the polarization properties of these targets, which are treated as calibration sources, cannot be accurately measured in advance. Polarization compensation is another method to reduce the effects of polarization aberrations. For systems with large FOV, however, it is challenging to compensate polarization aberrations and maintain wave aberrations simultaneously [22–25].

Low polarization system design is a good candidate for polarization-sensitive applications [26,27]. High-accuracy ellipsometers, spectrometers, interferometers, lithographic objective and radiometers require low polarization system design, which is the process of minimizing system polarization introduced by surface. Polarization aberrations of systems mainly depend on surface geometry and coating. The former is determined by optical design and the latter is by coating design. In most existing reports about low polarization system design, the coating is optimized [28,29]. Outstanding studies have been done by Chipman and Mahler et al. [29,30]. A space-based imager with low diattenuation was designed. Film thickness and material were optimized and controlled very carefully. However, it is difficult to achieve complex coating for optical systems with large aperture. Optical design, which plays important roles in polarization aberrations and is the necessary step to achieve low polarization, has not been described in detail yet. In this paper, a method based on genetic algorithms to design the initial configuration of low polarization on-axis three-mirror reflective optical systems is proposed. Wave aberrations, diattenuation and retardance would be optimized simultaneously.

The rest of this paper is arranged as follows. Basic principles of optical design of three-mirror reflective systems are shown in Section 2.

* Corresponding author.

E-mail address: luojingopt@ciomp.ac.cn (J. Luo).

In Section 3, the complexity and feasibility about designing low polarization three-mirror systems are analyzed. Detailed genetic algorithms used in this paper are described in Section 4. Several typical design results and examples are provided in Section 5. Some discussions and conclusions are summarized in Section 6.

2. Optical design of on-axis three-mirror reflective systems

Three-mirror reflective optical systems are composed of three mirrors: a primary mirror (PM), a secondary mirror (SM) and a tertiary mirror (TM) [31]. For three-mirror systems, there are seven free design parameters, i.e., K_1 , K_2 , K_3 , α_1 , α_2 , β_1 and β_2 . K_1 , K_2 and K_3 are the conic coefficients of PM, SM and TM, respectively. α_1 is the obscure ratio of SM to PM, α_2 is the obscure ratio TM to SM. β_1 and β_2 are the magnifications of SM and TM, respectively [32].

Assuming that the focal length of a three-mirror system is f' , based on the definition of magnification and obscure ratio, the expressions for the radii of curvature of different mirrors r_i and their corresponding separations d_i can be calculated according to the paraxial optical theory [33]:

$$\begin{cases} r_1 = \frac{2f'}{\beta_1\beta_2} \\ r_2 = \frac{2\alpha_1 f'}{(1+\beta_1)\beta_2} \\ r_3 = \frac{2\alpha_1\alpha_2 f'}{1+\beta_2} \end{cases}, \quad (1)$$

and

$$\begin{cases} d_1 = \frac{1-\alpha_1}{\beta_1\beta_2} f' \\ d_2 = \frac{\alpha_1(1-\alpha_2)f'}{\beta_2} \\ d_3 = \alpha_1\alpha_2 f' \end{cases}. \quad (2)$$

The relation between the third-order wave aberrations and the seven design parameters can be obtained by tracing the marginal and chief rays [32]

$$\begin{cases} S_I = S_I(K_1, K_2, K_3, \alpha_1, \alpha_2, \beta_1, \beta_2) \\ S_{II} = S_{II}(K_2, K_3, \alpha_1, \alpha_2, \beta_1, \beta_2) \\ S_{III} = S_{III}(K_2, K_3, \alpha_1, \alpha_2, \beta_1, \beta_2) \end{cases}, \quad (3)$$

where S_I is spherical aberration, S_{II} is astigmatism and S_{III} indicates coma. For the initial construction of on-axis three-mirror reflective systems, it is necessary to make the three wave aberrations as close to zero as possible. Hence, three equations can be built according to Eq. (3) and corresponding constraints are generated for the seven free design parameters, which means that the number of remaining free parameters is four. If focal plane is required to be flat, the fourth equation is

$$S_{IV} = \beta_1\beta_2 - \frac{\beta_2(1+\beta_1)}{\alpha_1} + \frac{1+\beta_2}{\alpha_1\alpha_2} = 0, \quad (4)$$

where S_{IV} is curvature of field. Obviously, there are three design parameters which are free if both Eqs. (3) and (4) are satisfied. It should be noted that the above equations are built to achieve good wave aberrations for three-mirror systems.

3. Complexity and feasibility

Genetic algorithms have been used widely to find good initial configurations for three-mirror reflective systems [32,34,35]. However, their optimization objectives are all good wave aberrations. In this paper, genetic algorithms is used to design low polarization three-mirror systems for the first time. There are big differences between wave aberrations and polarization aberrations [14,15,18]. As a result, different difficulties appear and different methods are adopted. In this section, we will introduce some considerations and analyses when we carry out this work.

3.1. Wave aberrations

For most imaging applications, wave aberrations are far more important than polarization aberrations. Before realizing low polarization systems, good wavefront performance must be achieved firstly. For three-mirror systems, there are seven free design parameters, i.e., K_1 , K_2 , K_3 , α_1 , α_2 , β_1 and β_2 . If spherical aberration, astigmatism and coma are eliminated, α_1 , α_2 , β_1 and β_2 are free. Fortunately, the structural outline of three-mirror systems depends entirely on the remaining four parameters [33], which is critical to achieve low polarization. Even though the focal plane is required to be flat, there are still three design parameters which are free. Hence, three-mirror reflective optical systems have the potential to realize low polarization with good wave aberrations.

3.2. Design parameter selection

Many global optimization algorithms including genetic algorithms have been used to design optical systems [32,35–37]. Choosing appropriate design parameters is critical to the efficiency and results of global optimization. The constructional parameters are often used as the design parameters [37,38]. The constructional parameters of on-axis three-mirror systems constitute the radius of curvature of mirrors r_1 , r_2 , r_3 , conic coefficients K_1 , K_2 , K_3 , and separations between the surfaces d_1 , d_2 , d_3 . The constructional parameters allow us to construct the systems or to model them in an optical design program directly. In addition, system parameters α_1 , α_2 , β_1 , β_2 , K_1 , K_2 and K_3 are also used as the design parameters in global optimization of three-mirror systems [32,35].

In this paper, our object is low polarization on-axis three-mirror systems with good wave aberrations. If the nine constructional parameters are selected as design parameters, systems with good wave aberrations should be found firstly. However, nine free parameters constitute so large search space that most computing resources would be used to find good wave aberrations. And then limited resources are left to search systems with low polarization. The probability of finding systems with both good wave aberrations and low polarization is very low. Hence, constructional parameters are not used as the design parameters in this paper.

In order to improve computing efficiency and avoid major resources being used to calculate systems with good wave aberrations, α_1 , α_2 , β_1 and β_2 are used as the four design parameters in this paper. According to the characteristics of three-mirror reflective optical systems, K_1 , K_2 , K_3 can be calculated by solving Eq. (3), and then spherical aberration, astigmatism and coma are eliminated directly. Hence, good wave aberrations can be achieved instantly. The constructional parameters can be obtained by solving Eqs. (1) and (2). It is noted that if field curvature is required to be eliminated, i.e., focal plane needs to be flat, there are three free design parameters α_1 , α_2 and β_1 . Once the free design parameters are determined, wave aberrations of the generated system would be obtained and qualified automatically, and only polarization aberrations need to be calculated and optimized.

3.3. Polarization ray-tracing

Polarization aberrations of an optical system can be obtained by polarization ray tracing [39]. However, the calculation process is rather complicated and much time would be spent. Avoiding polarization ray tracing was the focus of our considerations at the beginning. For reflective optical systems, smaller angle of incidence enables to realize lower polarization. Bigger radii of curvature of mirrors often have smaller incident angles. Hence, enlarging the radii of curvature of all the three mirrors seems to be a feasible solution to achieve low polarization. More importantly, polarization ray tracing can be avoided.

After careful considerations, however, this idea is infeasible. The fact is that it is hard to know the polarization aberration performance of

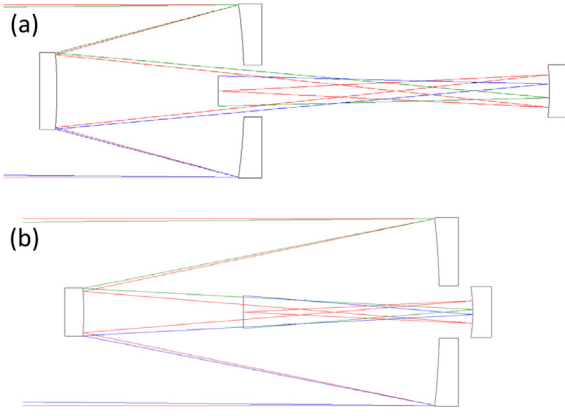


Fig. 1. Schematic diagram of two on-axis three-mirror systems (a) S1 and (b) S2.

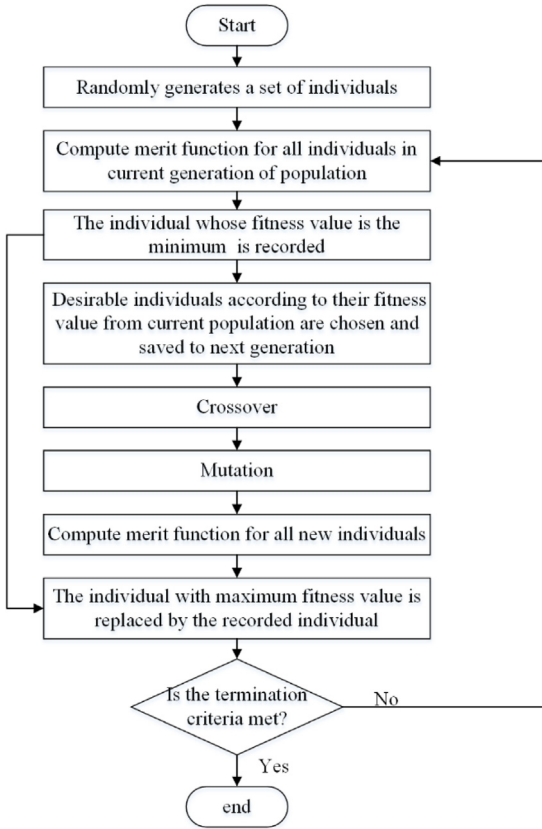


Fig. 2. Flow chart of the genetic algorithm.

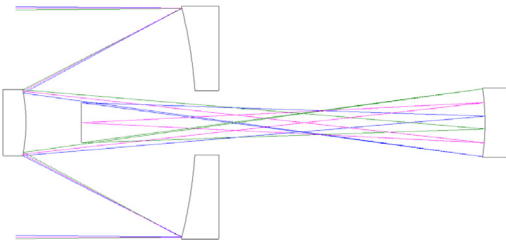


Fig. 3. Schematic diagram of a typical on-axis three-mirror reflective system.

a system only via the radii of curvature of mirrors. Let us illustrate this with an example. There are two on-axis three-mirror reflective systems

Table 1

Specifications of the two on-axis three-mirror systems.

Specifications	S1	S2
α_1	0.4195	0.2195
α_2	-0.4544	-0.5544
β_1	-2.5005	-2.5005
β_2	2.1479	1.6479
r_1	-372.3823	-485.3693
r_2	-260.3226	-177.5406
r_3	-121.1098	-91.9150
Polarization aberrations	2.67	1.72

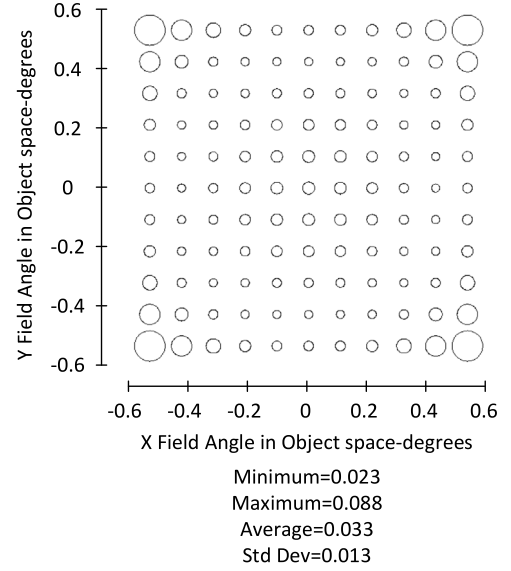


Fig. 4. RMS wavefront error vs field angle in object space.

shown in Fig. 1(a) and (b), respectively. The design parameters and radii of mirrors of the two systems are shown in Table 1. The absolute value of radius of PM in S1 is smaller than that of S2. However, the absolute values of radii of both SM and TM in S1 are bigger than the counterparts of S2. It is difficult to judge directly which one is with lower polarization aberrations. After polarization ray tracing, it is found that polarization aberrations of S1 is bigger than those of S2. Evidently, the relationship between polarization aberrations and radii of curvature of mirrors is complicated. Of course, polarization aberrations of a system would probably be lower if all the radii of curvature of mirrors are bigger. Hence, radii of curvature of mirrors cannot be used directly to design low polarization on-axis three-mirror systems. The polarization aberrations of a system should be calculated during the design process. In this paper, the three-dimensional polarization ray-tracing calculus is used [39].

As mentioned before, polarization ray tracing with high sampling density is time-consuming. Considering our design objects are on-axis systems, whose structures are rotationally symmetric and polarization aberrations are also rotationally symmetric [9], only quarter area of every system is analyzed by polarization ray tracing.

4. Genetic algorithms for low polarization optical system design

Genetic algorithms, which use principles inspired by nature to “evolve” toward a best solution, belong to global optimization algorithm that does not depend on the initial parameters. Genetic algorithms are well-suited for high-dimensional and highly nonlinear optimization problems [40]. In fact, genetic algorithm have been widely used to design optical systems including three-mirror systems [35,37]. Good optimization effects are obtained. Considering the effective design parameters are not continuous and the relationship between design

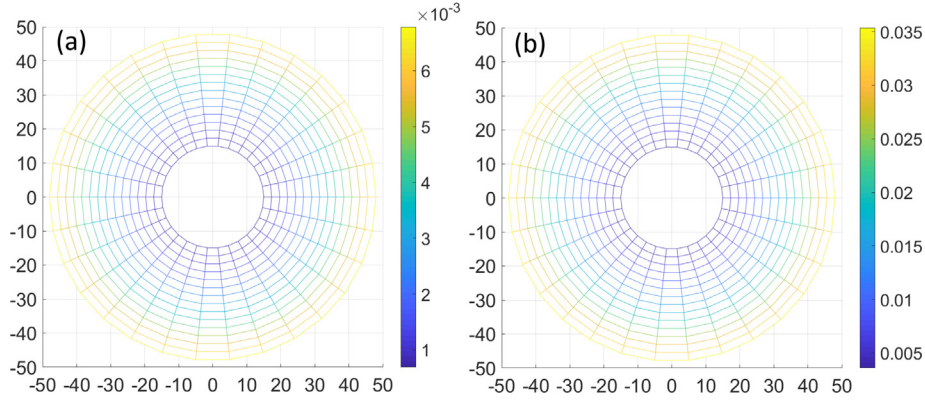


Fig. 5. Cumulative (a) diattenuation (dimensionless) map and (b) retardance (radians) map over the entrance pupil.

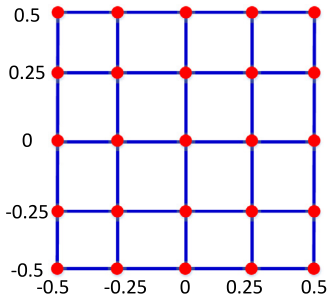


Fig. 6. The distribution of 25 FOVs involved in the calculation.

parameters and constructional parameters is highly nonlinear, genetic algorithm is chosen in this paper. Generally, a basic genetic algorithm includes five phases: 1. initialization, 2. selection, 3. crossover, 4. mutation, and 5. termination. The flow chart of the genetic algorithm used in this paper is shown in Fig. 2.

4.1. Coding mode

As mentioned in Section 3.2, the design parameters are α_1 , α_2 , β_1 and β_2 in this paper. The constructional parameters of three-mirror systems can be obtained by solving Eqs. (1) and (2). The advantage of our design parameter selection is that all three-mirror systems determined by the solved constructional parameters are with good wave aberrations. However, it is difficult to control the range of every constructional parameter via the design parameters. As a result, some systems characterized by the solved constructional parameters do not exist in reality, such as systems in which $d_2 < 0$. The design parameters that can generate effective optical systems are regarded as the effective design parameters. Unfortunately, it is found that effective design parameters are not always continuous. What is more, the relationship between design parameters and constructional parameters is highly nonlinear. Since the constructional parameters are obtained from the design parameters by solving equations, small differences in the design parameters sometimes lead to very different optical systems. Hence, the solution space should be searched finely, and an appropriate coding method is critical. After careful considerations and comparisons, decimal coding is chosen in this paper. The initial population is generated randomly in the solution space.

4.2. Merit function

Considering the goal of this paper is three-mirror optical systems with low polarization and good wave aberrations, the initial merit

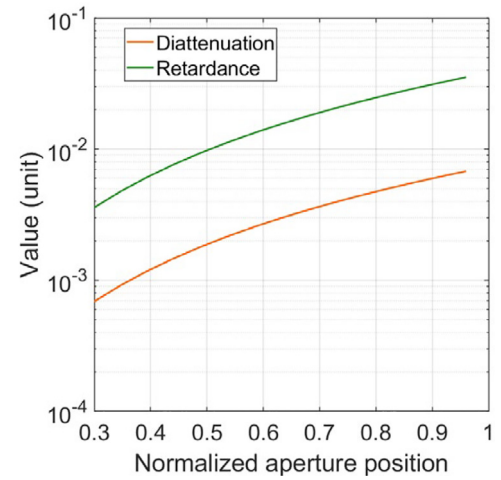


Fig. 7. Polarization aberrations along different aperture positions at one azimuth angle.

function is set to be

$$F = w_1 D + w_2 R + w_3 WFR, \quad (5)$$

where D means diattenuation, R is retardance, WFR is the RMS of wave aberrations. In Eq. (5), both diattenuation and retardance are involved. For some applications, only diattenuation or retardance is significant so that weight factor w_1 and w_2 can be changed to adapt to corresponding requirements. In this paper, we aim for diattenuation and retardance of optical systems to be small simultaneously. Considering the diattenuation is about one tenth of retardance in rad for a ray reflect from a plane coated aluminum [9], w_1 is set to be 10 while both w_2 and w_3 are 1 in this paper.

Three-mirror systems are generally customized. Hence, the merit function would be changed according to specific applications, such as compact structure, an intermediate image plane exists, flat focal plane, and so on. Different merit functions generate different optimal optical systems. Detailed analyses will be introduced later.

4.3. Selection method

As shown by Eq. (5), the merit function in this paper pursues the minimum fitness value. The fitness value is calculated for every individual. A specific number of individuals would be picked out randomly from current population and one individual whose fitness value is the minimum will be selected and preserved to the next generation of population. The operation is repeated until the next generation of population has the same number of individuals as current population.

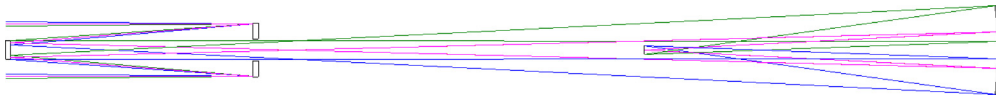


Fig. 8. Schematic diagram of the example 1.

Table 2

Main system parameters of on-axis three-mirror systems.

Specifications	Value
Focal length/mm	1000
Entrance pupil diameter/mm	100
FOV/°	1 × 1

4.4. Crossover and mutation

Due to the characteristics of optical design of three-mirror systems, the effective design parameters in solution space are highly discontinuous and nonlinear. Considering integer bits and the first decimal bits of the design parameters play more important roles than other decimal bits in solving effective constructional parameters, different crossover probabilities and mutation probabilities are used. Changes in the probability of the integer bit of the design parameters are lower than the counterparts of decimal bits. What is more, change probabilities of the first decimal bit are lower than the remaining decimal bits.

5. Examples and results

In order to show the performance of the genetic algorithms in low polarization three-mirror system design, several optimized results are presented in this section. Firstly, a typical on-axis three-mirror reflective optical system that has not been optimized for low polarization will be introduced and analyzed as a reference. Then, different low polarization systems are obtained in terms of different constraints and requirements via genetic algorithms. For comparison, the main system parameters of all three-mirror systems in this paper are set to be with the same values, as shown in Table 2. What is more, all systems in this paper are coated with barely metal aluminum, whose refractive index is $1.45+7.54i$ at 632.8 nm [41].

5.1. A typical on-axis three-mirror reflective system

A typical on-axis three-mirror reflective system is shown in Fig. 3, the focal length is 1000 mm and F number is 10. The free design parameters of the system are

$$[\alpha_1, \alpha_2, \beta_1] = [0.2702, -0.6519, -4.4152]. \quad (6)$$

The field curvature of the system is eliminate so that its focal plane is flat. Hence, the magnification of $\text{TM } \beta_2$ is not free and can be calculated via Eqs. (4) and (6). The intermediate image plane exists and locates on the right of the PM, which is critical to avoid secondary obstruction caused by the focal plane. The wave aberrations over $1^\circ \times 1^\circ$ field of view (FOV) are shown in Fig. 4. The average value of RMS of wave aberrations over all FOVs is 0.033λ (632.8 nm).

The polarization aberrations of the on-axis three-mirror system are analyzed. Cumulative diattenuation (dimensionless) and retardance (radians) maps over all the three mirrors in the system are obtained. Results are shown in Fig. 5(a) and (b), respectively. In order to get the polarization aberrations of the system over all FOVs, the system at 25 different FOVs is analyzed by polarization ray tracing. The distribution of these FOVs is shown in Fig. 6. It is noted that the polarization aberration at every point in Fig. 5 is the corresponding average value over the 25 FOVs. As shown in Fig. 5, the maximum diattenuation is $6.55\text{e-}3$ and the maximum retardance is $3.54\text{e-}2\text{ rad}$, which appear at the edge of the system. Both the diattenuation map and retardance map are rotationally symmetric [9]. Polarization aberrations along different aperture position at one azimuth angle would be picked out and compared, as shown in Fig. 7.

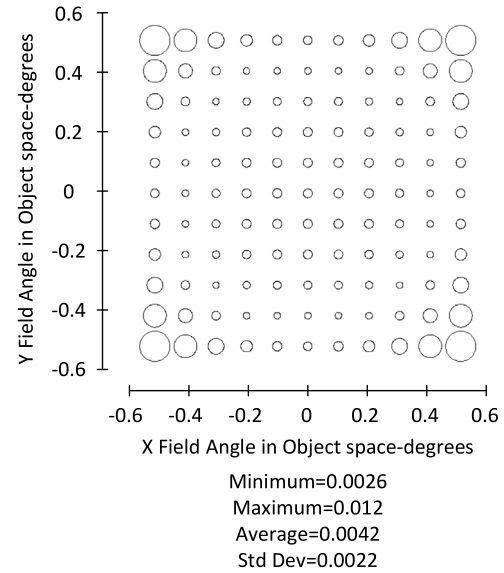


Fig. 9. RMS wavefront error vs field angle in object space of the example 1.

5.2. Example 1

Let us start the low polarization on-axis three-mirror reflective systems design by the genetic algorithm. The merit function is shown as Eq. (5). Only polarization aberrations and wave aberrations are involved without other constraints. An optimized result is shown in Fig. 8, whose free design parameters are

$$[\alpha_1, \alpha_2, \beta_1, \beta_2] = [0.2777, -2.4325, -3.0818, 0.5045]. \quad (7)$$

As shown in Fig. 9, wave aberrations of the system are so good that the average RMS of wave aberrations over all FOVs is only 0.0042λ (632.8 nm). Cumulative polarization aberrations of the system are obtained. Diattenuation and retardance of the system are compared to the counterparts of the normal system shown in Fig. 3, respectively. Results are shown in Fig. 10(a) and (b). Obviously, polarization aberrations of the system in Fig. 8 are drastically reduced after the low polarization design. The maximum diattenuation is reduced from $6.55\text{e-}3$ to $1.85\text{e-}4$. The maximum retardance is reduced from $3.54\text{e-}2$ to $1.16\text{e-}3$, respectively. The polarization aberrations of the example 1 are only one-thirtieth of the normal system shown in Fig. 3.

The results shown in Fig. 10 show that $\alpha_1, \alpha_2, \beta_1$ and β_2 enable to provide enough space to search and achieve low polarization three-mirror reflective optical systems. Hence, the idea proposed in this paper is feasible. However, the structure size of the system shown in Fig. 8 is rather long. The length of the system is 1889 mm, which is the distance between the SM and the TM. A parameter η is defined as the ratio between the length L of an optical system and the diameter D of the clear aperture, i.e.,

$$\eta = \frac{L}{D}, \quad (8)$$

where L is the maximum length between d_1 and d_2 , i.e.,

$$L = \max \{|d_1|, |d_2|\}, \quad (9)$$

where d_1 is the separation from PM to SM and d_2 is the separation from SM to TM. For this system $\eta = 18.89$. A compact optical system is

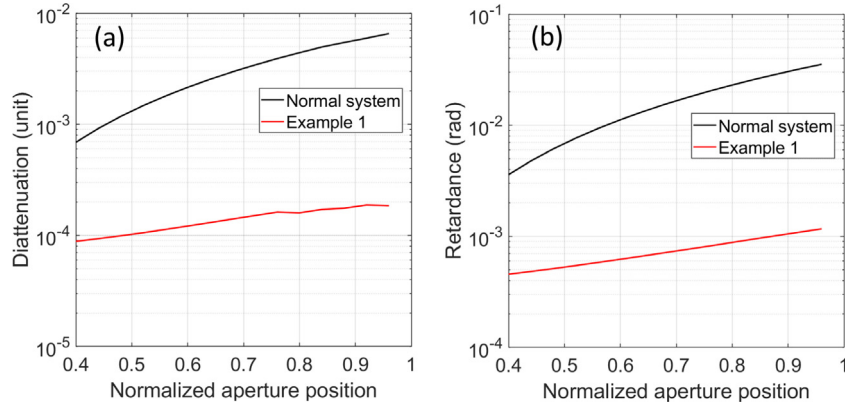


Fig. 10. (a) Diattenuation and (b) retardance along different aperture positions at one azimuth angle.

desirable in many applications. Hence, structure size should be added into the merit function.

5.3. Example 2

As shown by the example 1, if the merit function contains only polarization aberrations and wave aberrations, systems with very low polarization aberrations and good wave aberrations can be found by genetic algorithms. However, these systems would probably be very long, which makes them are not with practical significance. In this section, the ratio η of three-mirror systems is added into the merit function. What is more, the intermediate image plane is required to exist and locate at the right of the PM, which is critical to avoid secondary obstruction. Hence, the merit function in this section becomes

$$F = w_1 D + w_2 R + w_3 WFR + w_4 \eta + w_5 IMG_1, \quad (10)$$

where η characterizes the length of systems and IMG_1 relates to the intermediate image plane.

In terms of the new merit function shown in Eq. (10), optical systems with low polarization aberrations are searched using the genetic algorithm. The merit function variation versus evolving generations is shown in Fig. 11. An optimized system is shown in Fig. 12, whose free design parameters are

$$[\alpha_1, \alpha_2, \beta_1] = [0.2333, -0.9049, -4.0782]. \quad (11)$$

The RMS of wave aberrations over all FOVs is shown in Fig. 13. Obviously, the wave aberrations of the system are very good, and its focal plane is flat. The ratio η of the system is 4.1, which is much smaller than that of the example 1. The polarization aberrations of the system are shown in Fig. 14. The maximum diattenuation is 1.29×10^{-3} and the maximum retardance is 7.41×10^{-3} , which are about one fifth of the counterparts of the normal system and larger than those of the example 1. Different weight factors w_4 in Eq. (10) give rise to different optimized results. If the weight factor w_4 is decreased, systems with lower polarization aberrations can be found while their structure sizes usually be longer, such as the example 1 in which $w_4 = 0$. Different weight factors can be set by designers according to their own requirements.

It should be noted that the TM is obscured by the focal plane in Fig. 12. However, the constraints about intermediate image plane have been added into the merit function, as the IMG_1 in Eq. (10). Hence, the intermediate image plane of the system in Fig. 12 exists and locates at the right of the PM. As a result, it is easy to avoid secondary obstruction by adding a plane mirror in the neighborhood of the intermediate image plane [31]. Of course, the additional plane mirror has impacts on the polarization aberrations of the on-axis system. Two crossed fold mirrors would be better [23]. Considering the focus of the paper is the initial configuration of on-axis three-mirror systems, further discussions about additional plane mirrors to avoid secondary obstruction would not be carried out in this paper.

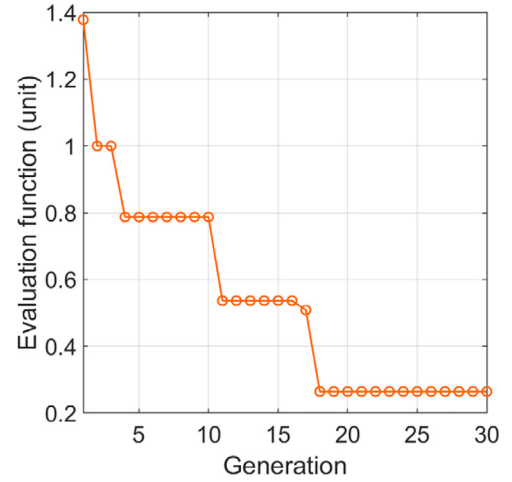


Fig. 11. Merit function variation curve.

5.4. Example 3

The focal planes of all the aforementioned systems are flat. If this requirement is removed, the design parameter β_2 becomes free and there are four free design parameters. The merit function is identical to Eq. (10). Some new systems are obtained by the genetic algorithm and an example is shown in Fig. 15, whose free design parameters are

$$[\alpha_1, \alpha_2, \beta_1, \beta_2] = [0.3966, -0.5512, -1.5898, 1.3296]. \quad (12)$$

The wave aberrations of the $[0^\circ, 0^\circ]$ FOV is 0.004λ . The ratio η is 4.6, which is close to that of the example 2. The intermediate image plane also exists and locates at the right of the PM. Hence, secondary obstruction can be avoided, as mentioned in the last part of Section 5.3. As shown in Fig. 16, the maximum diattenuation and retardance of the system are 4.38×10^{-4} and 2.45×10^{-3} , respectively, which are smaller than the counterparts of the example 2. One more free design parameter helps the example 3 to achieve lower polarization with similar system length.

5.5. Example 4

If the intermediate image plane does not exist, the merit function becomes

$$F = w_1 D + w_2 R + w_3 WFR + w_4 \eta. \quad (13)$$

A compact system with flat focal plane is obtained by the genetic algorithm, as shown in Fig. 17. The free design parameters are

$$[\alpha_1, \alpha_2, \beta_1] = [0.3799, 0.5226, -3.3890]. \quad (14)$$

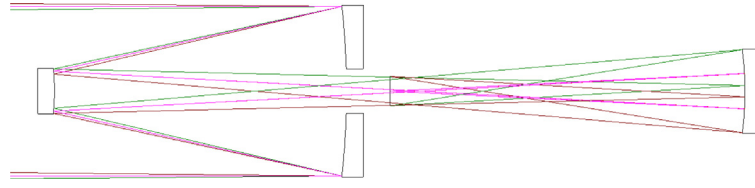


Fig. 12. Schematic diagram of example 2.

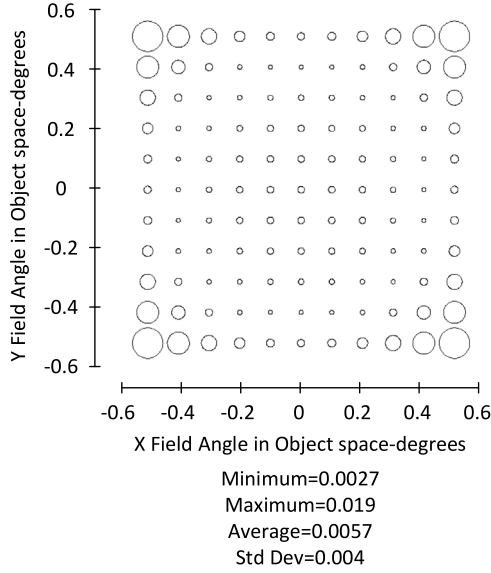


Fig. 13. RMS wavefront error vs field angle in object space of example 2.

As shown in Fig. 18, the average RMS of wave aberrations over all FOVs is 0.0091λ . The ratio η of the system is only 2.9. Polarization aberrations of the system are obtained and shown in Fig. 19. The maximum diattenuation and retardance of the system are $4.35\text{e-}4$ and $2.31\text{e-}3$, respectively, which are close to the counterparts of the example 3. Reducing constraint about the intermediate image plane is helpful to achieve compact three-mirror systems with low polarization.

In order to show the design results more clearly, main parameters and properties of these systems are summarized in Table 3. The secondary obstructions of original system, example 2 and example 3 can be avoided because the intermediate image planes in all the three systems exist and locate at the right of the PM. Detailed explanations can be found in the last part of Section 5.3.

6. Discussions and conclusions

Thanks to be with seven free design parameters, three-mirror reflective systems have good potential to achieve low polarization. After good wave aberrations are met, there are four design parameters are free. If the focal plane is required to be flat, three parameters can be free. In this paper, it is shown that polarization aberrations of on-axis three-mirror systems can be optimized and reduced by genetic algorithms based on these free parameters.

If only polarization aberrations and wave aberrations are included in the merit function, three-mirror systems with both very low polarization and good wave aberrations can be obtained via the genetic algorithm. However, the lengths of the design results are usually so long that they are with obvious disadvantages in some engineering applications. After the length ratio η is added into the merit function, a new balance is built and systems with low polarization aberrations and shorter structural dimensions are found.

Besides length, there are many other factors that affect on-axis three-mirror reflective systems, such as obscure ratio, secondary obstruction, flat focal plane, and so on. To ensure the design results to be with practical significance, more constraints are forced to be involved in the merit function. However, increasing constraints would affect the performance of low polarization optimization if the number of free design parameters does not increase. The example 2 is a good design result in which all the aforementioned constraints are involved. A good balance is achieved between polarization aberrations and these constraints. The ratio η of the system is 4.1. The maximum diattenuation is $1.29\text{e-}3$ and the maximum retardance is $7.41\text{e-}3$. Of course, lower polarization aberrations can be obtained if constraints are reduced, such as example 3 and example 4.

More free design parameters are helpful. It is found that polarization aberrations of the optimized results in which β_2 is free are very close to those in which intermediate image plane are not required. Increasing the number of mirrors, free-form surface, tilt angles of mirrors are good choices to design better low polarization optical systems.

The method proposed in this paper can be used widely to design other types of optical systems that demand low polarization. The polarization aberrations of off-axis systems are usually larger than on-axis ones. Hence, it is more necessary for off-axis systems to perform

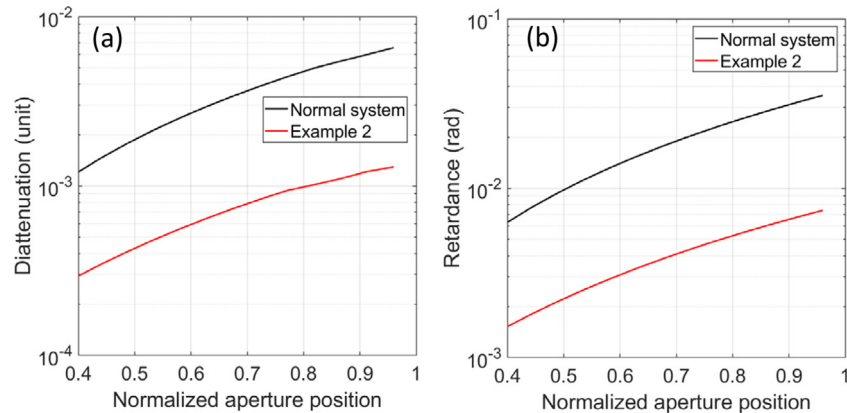


Fig. 14. (a) Diattenuation and (b) retardance along different aperture positions at one azimuth angle.

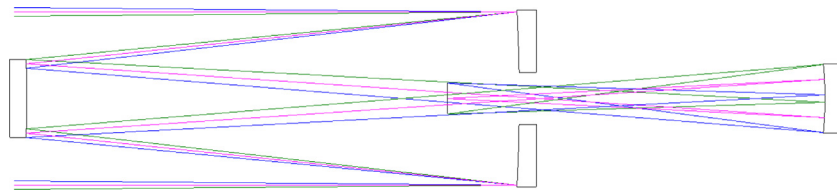


Fig. 15. Schematic diagram of example 3.

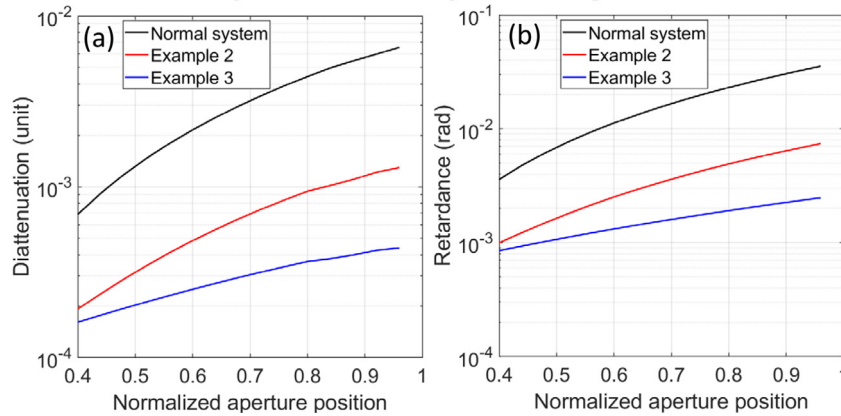


Fig. 16. (a) Diattenuation and (b) retardance along different aperture positions at one azimuth angle.

Table 3

Main parameters of the designed examples.

Case	Free parameters	η	WFR@FOV	D	R	Secondary obstruction
Original	$[\alpha_1, \alpha_2, \beta_1]$	2	$0.033\lambda@1^\circ \times 1^\circ$	$6.55e-3$	$3.54e-2$	Can be avoided
Example 1	$[\alpha_1, \alpha_2, \beta_1, \beta_2]$	18.8	$0.0042\lambda@1^\circ \times 1^\circ$	$1.85e-4$	$1.16e-3$	Can be avoided
Example 2	$[\alpha_1, \alpha_2, \beta_1]$	4.1	$0.0057\lambda@1^\circ \times 1^\circ$	$1.29e-3$	$7.41e-3$	Can be avoided
Example 3	$[\alpha_1, \alpha_2, \beta_1, \beta_2]$	4.6	$0.004\lambda@0^\circ \times 0^\circ$	$4.38e-3$	$2.45e-3$	Can be avoided
Example 4	$[\alpha_1, \alpha_2, \beta_1]$	2.9	$0.0091\lambda@1^\circ \times 1^\circ$	$4.35e-4$	$2.31e-3$	Has been avoided

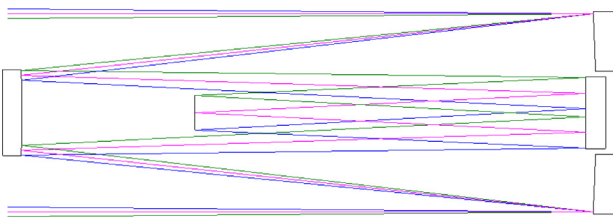


Fig. 17. Schematic diagram of example 4.

low polarization design. What is more, the decenter and tilt of mirrors in off-axis systems would provide more free design parameters to low polarization optimization. This would be one of the focuses of our future work.

Funding

This research is supported by the National Natural Science Foundation of China (12003033); National Key Research and Development Program of China (2021YFC2802100).

Declaration of competing interest

The authors declare that they have no known competing financial interests or personal relationships that could have appeared to influence the work reported in this paper.

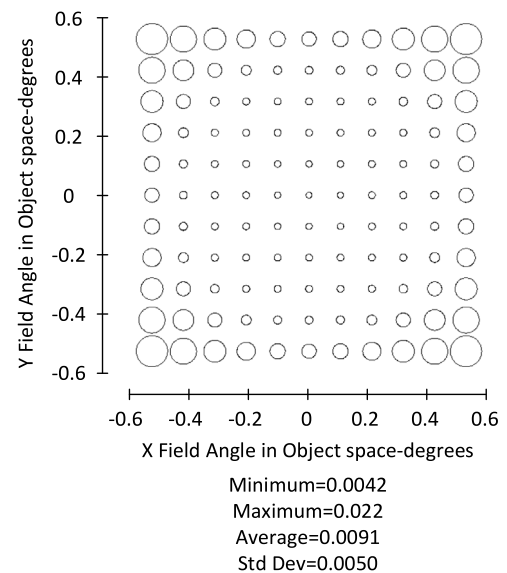


Fig. 18. RMS wavefront error vs field angle in object space of the example 4.

Data availability

Data will be made available on request.

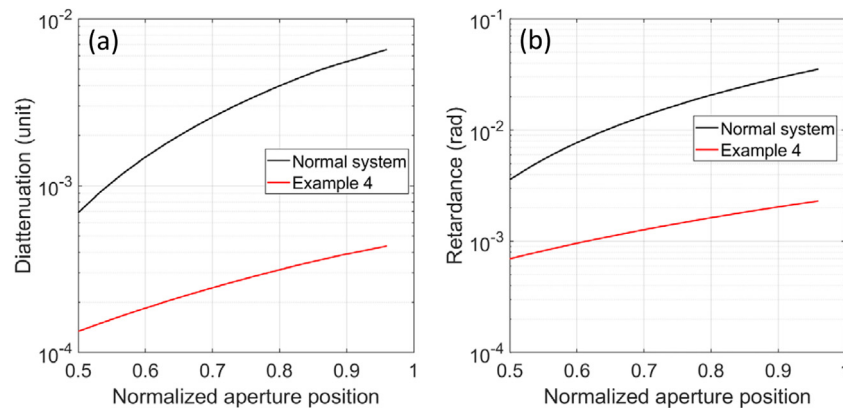


Fig. 19. (a) Diattenuation and (b) retardance along different aperture positions at one azimuth angle.

References

- [1] J.P. Gardner, J.C. Mather, M. Clampin, R. Doyon, G.S. Wright, The James Webb space telescope, *Space Sci. Rev.* 123 (2006) 485–606.
- [2] S. Martin, M. Rud, P. Scowen, D. Stern, J. Nissen, J. Krist, HabEx space telescope optical system, *Proc. SPIE* 10398 (2017) 1039805.
- [3] G.R. Laureijs, J. Amiaux, S. Arduini, J.-L. Augueres, J. Brinchmann, R. Cole, M. Cropper, C. Dabin, L. Duvet, A. Ealet, Euclid definition study report, 2011, [arXiv:1110.3193](https://arxiv.org/abs/1110.3193).
- [4] H. Tang, M. Rodgers, B. Creager, J. Krist, J. McGuire, K. Patterson, M. Rud, F. Shi, F. Zhao, The WFIRST coronagraph instrument phase B optical design, *Proc. SPIE* 11117 (2019) 111170C.
- [5] Y. Gong, X.W. Liu, Y. Cao, X. Chen, Z. Fan, R. Li, X. Li, Z. Li, X. Zhang, H. Zhan, Cosmology from the Chinese space station optical survey (CSS-OS), *Astrophys. J.* 883 (2) (2019) 203.
- [6] John D. Mill, Robert R. O'Neil, Stephan Price, J. Gerald, Midcourse space experiment: Introduction to the spacecraft, instruments, and scientific objectives, *J. Spacecr. Rockets* 31 (5) (1994) 900–907.
- [7] A. Boccaletti, J. Schneider, W. Traub, P.-O. Lagage, D. Stam, R. Gratton, J. Trauger, K. Cahoy, F. Snik, P. Baudoz, SPICES: Spectro-polarimetric imaging and characterization of exoplanetary systems from planetary disks to nearby super earths, *Exp. Astron.* 34 (2012) 355–384.
- [8] B. Sang, J. Schubert, S. Kaiser, V. Mogulsky, C. Neumann, K.P. Förster, S. Hofer, T. Stuffer, H. Kaufmann, A. Müller, The EnMAP hyperspectral imaging spectrometer: Instrument concept, calibration, and technologies, *Proc. SPIE* 7086 (2008) 708605.
- [9] J. Luo, C. You, X. He, X. Zhang, Comparisons between an on-axis three-mirror anastigmat telescope and an off-axis one: Polarization aberrations, *Appl. Opt.* 60 (22) (2021) 6438–6447.
- [10] D.M. Harrington, S.R. Sueoka, Polarization modeling and predictions for Daniel K. Inouye solar telescope part 1: Telescope and example instrument configurations, *J. Astron. Telesc. Instrum. Syst.* 3 (2017) 018002.
- [11] F.C.M. Bettonvil, M. Collados, A. Feller, B.F. Gelly, C.U. Keller, T.J. Kentischer, A.L. Ariste, O. Pleier, F. Snik, H. Socas-Navarro, The polarization optics for the European solar telescope (EST), *Proc. SPIE* 7735 (2010) 773561.
- [12] J. Breckinridge, M. Kupinski, J. Davis, B. Daugherty, R. Chipman, Terrestrial exoplanet coronagraph image quality: Study of polarization aberrations in Habex and LUVOIR update, *Proc. SPIE* 10698 (2018) 106981D.
- [13] M.R. Bolcar, LUVOIR telescope design overview, 2016.
- [14] R.A. Chipman, Polarization Aberrations, University of Arizona, 1987.
- [15] R.A. Chipman, G. Young, W.S.T. Lam, Polarized Light and Optical Systems, CRC Press, 2018.
- [16] S. Banerjee, Optical Design for Considering Polarization Effects Due to Reflective Surfaces, Utsunomiya University, 2020.
- [17] J. Luo, X.U. He, K. Fan, X. Zhang, Effects of polarization aberrations in an unobscured off-axis space telescope on its PSF ellipticity, *Opt. Express* 28 (25) (2020).
- [18] J.B. Breckinridge, W.S.T. Lam, R.A. Chipman, Polarization aberrations in astronomical telescopes: The point spread function, *Publ. Astron. Soc. Pac.* 127 (2015) 445.
- [19] H.H. Schwarzer, F. Blechinger, A.S. Menardi, Polarization monitoring device for the high-resolution imaging spectrometer (HRIS), *Proc. SPIE* 2480 (1995) 180–185.
- [20] A.J. Brown, T.I. Michaels, S. Byrne, W. Sun, T.N. Titus, A. Colaprete, M.J. Wolff, G. Videen, C.J. Grund, The case for a modern multiwavelength, polarization-sensitive LIDAR in orbit around Mars, *J. Quant. Spectrosc. Radiat. Transf.* 153 (2015) 131–143.
- [21] C.A. Hostetler, Z. Liu, J. Reagan, M. Vaughan, D. Winker, M. Osborn, W. Hunt, K. Powell, C. Treppe, CALIOP algorithm theoretical basis document—part 1: Calibration and level 1 data products, PC-SCI-202 part 1, 2.0, 2006.
- [22] J.M. Davis, Polarization Aberrations in Coronagraphs, The University of Arizona, 2019.
- [23] W.S.T. Lam, R. Chipman, Balancing polarization aberrations in crossed fold mirrors, *Appl. Opt.* 54 (11) (2015) 3236–3245.
- [24] L.J. Cox, The compensation of instrumental polarization by inclined mirrors, *Mon. Not. R. Astron. Soc.* 176 (1976) 525–532.
- [25] D. Sabatke, J.S. Knight, M.R. Bolcar, Polarization ray tracing and polarization aberration compensation in reflective, astronomical telescopes, *Proc. SPIE* 10743 (2018) 1074307.
- [26] Y. Wang, X. Tan, K. Tatsuno, X. Liu, Y. Li, K. Liu, Polarization aberration control for hyper-NA lithographic projection optics at design stage, *Proc. SPIE* 9618 (2015) 96180H.
- [27] N. Kita, Technique to manage polarization aberrations, *Opt. Rev.* 16 (2009) 305–312.
- [28] K. Balasubramanian, D.J. Hoppe, P.Z. Mouroulis, L.F. Marchen, S.B. Shaklan, Polarization compensating protective coatings for TPF-coronagraph optics to control contrast degrading cross polarization leakage, *Proc. SPIE* 5905 (2005) 59050H.
- [29] A.B. Mahler, P.K. Smith, R.A. Chipman, Low polarization optical system design, *Proc. SPIE* 6682 (2007) 66820V.
- [30] A.-B. Mahler, N.A. Raouf, P.K. Smith, S.C. McClain, R.A. Chipman, Minimizing instrumental polarization in the multiangle SpectroPolarimetric imager (MSPI) using diattenuation balancing between the three mirror coatings, *Proc. SPIE* 7013 (2008) 701355.
- [31] P.N. Robb, Three-mirror telescopes: Design and optimization, *Appl. Opt.* 17 (17) (1978) 2677–2685.
- [32] L. Jun, W. Huang, F. Hongjie, A novel method for finding the initial structure parameters of optical systems via a genetic algorithm, *Opt. Commun.* 361 (2016) 28–35.
- [33] J. Pan, The Design, Manufacture and Test of the Aspherical Optical Surfaces, Suzhou University, 2004.
- [34] K. Höschel, V. Lakshminarayanan, Genetic algorithms for lens design: A review, *J. Opt.* 48 (1) (2019) 134–144.
- [35] Z. Mi, Z. Li, X. Zhang, Construction of a compact off-axis three-mirror reflective system, *Appl. Opt.* 61 (9) (2022) 2424–2431.
- [36] C.C. Reichert, T. Gruhonic, A.M. Herkommer, Development of an open source algorithm for optical system design, combining genetic and local optimization, *Opt. Eng.* 59 (5) (2020) 055111.
- [37] C. Cao, S. Liao, Z. Liao, Y. Bai, Z. Fan, Initial configuration design method for off-axis reflective optical systems using nodal aberration theory and genetic algorithm, *Opt. Eng.* 58 (10) (2019) 1.
- [38] S. Pal, L. Hazra, Structural design of optically compensated zoom lenses using genetic algorithm, *Proc. SPIE* 7429 (2009) 742910.
- [39] G. Yun, K. Crabtree, R.A. Chipman, Three-dimensional polarization ray-tracing calculus I: definition and diattenuation, *Appl. Opt.* 50 (18) (2011) 2855–2865.
- [40] N. HesamMahmoudiNezhad, Optical System Optimization using Genetic Algorithms, Delft University of Technology, 2014.
- [41] Raki, D. Aleksandar, Algorithm for the determination of intrinsic optical constants of metal films: Application to aluminum, *Appl. Opt.* 34 (22) (1995) 4755–4767.